MOLECULAR AND CELLULAR BIOLOGY, Mar. 2009, p. 1538–1553 Vol. 29, No. 6
0270-7306/09/$08.00+0 doi:10.1128/MCB.01375-08

Convergent Functional Genomics of Oligodendrocyte Differentiation Identifies Multiple Autoinhibitory Signaling Circuits[▽]†

Rosanna Pescini Gobert, Lara Joubert, Marie-Laure Curchod, Catherine Salvat, Isabelle Foucault, Catherine Jorand-Lebrun, Marc Lamarine, Hélène Peixoto, Chloé Vignaud, Christèle Frémaux, Thérèse Jomotte, Bernard Françon, Chantal Alliod, Lilia Bernasconi, Hadi Abderrahim, Dominique Perrin, Agnes Bombrun, Francisca Zanoguera, Christian Rommel,‡ and Rob Hooft van Huijsduijnen*

Merck Serono SA, 1211 Geneva, Switzerland

Received 29 August 2008/Returned for modification 11 December 2008/Accepted 22 December 2008

Inadequate remyelination of brain white matter lesions has been associated with a failure of oligodendrocyte precursors to differentiate into mature, myelin-producing cells. In order to better understand which genes play a critical role in oligodendrocyte differentiation, we performed time-dependent, genome-wide gene expression studies of mouse Oli-neu cells as they differentiate into process-forming and myelin basic protein-producing cells, following treatment with three different agents. Our data indicate that different inducers activate distinct pathways that ultimately converge into the completely differentiated state, where regulated gene sets overlap maximally. In order to also gain insight into the functional role of genes that are regulated in this process, we silenced 88 of these genes using small interfering RNA and identified multiple repressors of spontaneous differentiation of Oli-neu, most of which were confirmed in rat primary oligodendrocyte precursors cells. Among these repressors were CNP, a well-known myelin constituent, and three phosphatases, each known to negatively control mitogen-activated protein kinase cascades. We show that a novel inhibitor for one of the identified genes, dual-specificity phosphatase DUSP10/MKP5, was also capable of inducing oligodendrocyte differentiation in primary oligodendrocyte precursors. Oligodendrocytic differentiation feedback loops may therefore yield pharmacological targets to treat disease related to dysfunctional myelin deposition.

Demyelination and/or incomplete remyelination, followed by axonal loss and neuronal death, is associated with several neurodegenerative disorders, including multiple sclerosis (37), Pelizaeus-Merzbacher disease, and spastic paraplegia type 2 (16), while myelin abnormalities are also seen for psychiatric disorders, including major depression (2), schizophrenia, and autism (reviewed in reference 10). In humans, the central neural system consists of an unusually high proportion (50%) of white matter, which is normally maintained by proliferating, migrating, and remyelinating oligodendrocytes (10). However, in, for instance, secondary progressive multiple sclerosis, at a stage where the autoimmune insult has abated, myelin degeneration continues. This insufficiency of myelin repair has been attributed to a failure of oligodendrocyte precursors to differentiate (11, 20).

In order to better understand which genes play a role in multiple sclerosis, a number of proteomic (13), genomic (25, 29), and genetic (35) approaches have been utilized. However, diseased lesions consist of different admixtures (e.g., contain immune and glia infiltrates) of cell types compared to controls, so such postmortem samples may present differential cell, rather than gene or protein, expression. Therefore, understanding how such genes fit into pathophysiological processes (and in which) is problematic. From population genetic surveys thus far, only a few genes have been found to be associated with multiple sclerosis (31).

Based on these considerations, we chose to examine genome-wide gene expression changes in a murine oligodendroglial precursor cell line, Oli-neu (18), as these cells underwent differentiation into myelin basic protein (MBP)-producing cells. Even for a pure cell line, this type of transition is typically associated with changes in the expression of thousands of genes, by itself providing little meaningful information. We therefore decided to look at oligodendrocyte differentiation as induced by different agents, in the hope that from this combined data set one might extract "core genes" whose modulation is closely linked to the differentiation process. The enriched set of genes was further evaluated for their functional involvement in the differentiation process.

MATERIALS AND METHODS

Cells, media, and reagents. Oli-Neu cells were maintained in Dulbecco modified Eagle medium (DMEM)–F-12 (Invitrogen catalog no. 21331) supplemented with 50 μg of apo-transferrin (Sigma T-1147)/ml, 5 ng of sodium selenite (Sigma S-9133)/ml, 5 μg of insulin (Sigma I-0516)/ml, 100 μM putrescine (Sigma P-7505), 22 nM progesterone (Sigma P-7556), 0.5 nM T3 (Sigma T-6397), 1% horse serum (Invitrogen catalog no. 26050), 1% penicillin-streptomycin (Invitrogen catalog no. 15070), 2 mM glutamine (Invitrogen catalog no. 25030), 0.1% sodium bicarbonate (Invitrogen catalog no. 25080), and 15 mM HEPES (Invitrogen catalog no. 15630).

* Corresponding author. Mailing address: Merck Serono S.A., 9, Chemin des Mines, 1211 Geneva, Switzerland. Phone: 41 22 4143000. Fax: 41 22 7946965. E-mail: rob.hooft@merckserono.net.

† Supplemental material for this article may be found at http://mcb.asm.org/.

‡ Present address: Intellikine, Inc., 10931 North Torrey Pines Road, La Jolla, CA 92037.

▽ Published ahead of print on 12 January 2009.

Differentiation medium was composed of DMEM–F-12 supplemented with 50 μg of apo-transferrin/ml, 5 ng of sodium selenite/ml, 100 μM putrescine, 130 nM progesterone, 200 nM T3, 1% horse serum, 1% penicillin-streptomycin, 2 mM glutamine, 0.1% sodium bicarbonate, and 15 mM HEPES. Chemical treatments for microarray analysis included insulin at 10 μg/ml, 10 μM forskolin (Sigma F6886), 1 μM 13-*cis*-retinoic acid (LKT Laboratories R1779), 1 μM dexamethasone (Sigma D4902), and 1 μM PD174256 (Alexis ALX-270-323).

OPC isolation. Cortical oligodendrocyte precursors (OPCs) were purified from newborn Oncins France strain A rats. Isolated cortex was roughly dissociated with a scalpel and then incubated 10 min at 37°C in 10 ml of 1× Hanks balanced salt solution (Invitrogen catalog no. 14025)–0.01% trypsin (Invitrogen catalog no. 25300)–0.0024% DNase (Sigma D-5025). After centrifugation at 800 rpm for 5 min, the pellet was resuspended by pipetting in 2 ml of DMEM (Invitrogen catalog no. 31966)–1% penicillin-streptomycin–20% fetal bovine serum (Invitrogen catalog no. 10108), filtered through a 70-μm-pore-size cell strainer (BD-352350), and centrifuged again at 800 rpm for 10 min. One cortex per 75-cm^2 poly-D-lysine flask (BD-356537) was put in culture in DMEM supplemented with 20% fetal calf serum. The medium was changed every 3 days. At day 10, flasks were shaken for 1 h at 150 rpm, and the medium (containing the microglia) was removed. Then, 10 ml of fresh medium was added, and the flasks were shaken overnight at 280 rpm.

After filtration through a 150-μm-pore-size Nitex filter, the OPCs were counted and plated at the required density on poly-D-lysine in SATO serum-free medium composed of DMEM and 60 μg of *N*-acetylcysteine (Sigma A-9165), 5 μg of insulin (Sigma I-0516), 10 ng of biotin (Sigma B-4639), 20 ng of forskolin (Sigma F-6886), 100 μg of bovine serum albumin (Sigma A-4161), 100 μg of apo-transferrin (Sigma T-1147), 60 ng of progesterone (Sigma P-8783), 16 μg of putrescine (Sigma P-5780), and 40 ng of $NaSeO_3$ (Sigma S-9133)/ml.

RNA interference (RNAi) experiments. Annealed small interfering RNA (siRNA) duplexes (1 nM) were introduced into cells by using INTERFERin transfection reagent (catalog no. 409-10; Polyplus Transfection, Inc.). Transfection complexes were prepared in OptiMEM medium (Invitrogen catalog no. 51985) for 15 min at room temperature according to the manufacturer's instructions. The complexes were added to the cell suspension, and the cells were grown for 72 h.

RNA extraction and qPCR analysis. For the microarrays, total RNA extraction and DNase digestion were performed according to the manufacturer's instructions (RNeasy minikit; Qiagen). Nucleic acid concentrations of the samples were determined by using a NanoDrop spectrophotometer. Concentration and quality of the samples were confirmed by Bioanalyzer 2100 (Agilent Technologies). For all other quantitative (real-time) PCR (qPCR) assays, total RNA was prepared with TRIzol reagent (Invitrogen catalog no. 15596) according to the manufacturer's protocol. A total of 1 μg of total RNA was used as a template for reverse transcription with Superscript III (Invitrogen catalog no. 18080) and a 1:1 mix of oligo$(dT)_{20}$ (Invitrogen catalog no. 18418) and random primers (Invitrogen catalog no. 48190). cDNA was then diluted 50-fold, and real-time PCR was performed in triplicates using the QuantiFast SYBR green PCR master mix (Qiagen catalog no. 204054) and the respective QuantiTect primer assays.

Microarray procedure. A one-cycle eukaryotic target labeling assay (one-cycle target labeling and control reagents; Affymetrix catalog no. P/N 900493) was used to produce fragmented biotinylated cRNA from total RNA as described in the standard Affymetrix protocol (P/N 701021 Rev.5).

In this study, 3 μg of total RNA isolated were first reverse transcribed using a T7-oligo(dT) promoter primer in the first-strand cDNA synthesis reaction. After RNase H-mediated second-strand cDNA synthesis, the double-stranded cDNA was purified and served as a template in the subsequent in vitro transcription reaction. The in vitro transcription reaction was carried out in the presence of T7 RNA polymerase and a biotinylated nucleotide analog-ribonucleotide mix for cRNA amplification and biotin labeling. The biotinylated cRNA targets were then cleaned up, an aliquot of 20 μg was fragmented, and finally 15 μg was hybridized to a GeneChip Mouse Genome 430 2.0 array (Affymetrix, P/N 900495, 900496, and 900497). Chips were washed and labeled in a fluidics station, using protocol EuKGE-WS2v_45 After scanning, CEL files were analyzed by using GCOS software to check poly(A) and hybridization controls.

Data analysis. Analysis of the microarray experiment was carried using Resolver software from Rosetta. Differentially expressed genes were analyzed comparing each treatment and time point versus the respective time-matched untreated samples. Quality control measures were performed by using a two-dimensional agglomerative Resolver hierarchical clustering analysis (HCA) procedure using z-score transformed intensity experiments with a cosine correlation similarity measure, and Ward's minimum variance heuristic criteria were applied on two probe sets selections for untreated, dexamethasone, retinoic acid, and PD174265 conditions at 10 h and 72 h.

GCOS and MAS5.0 software from Affymetrix were in the range recommended by the manufacturer. The intensity profile pipeline from Rosetta was used to create an intensity (expression) profile for each sample. Then, the intensity experiment pipeline from Rosetta was used to derive, from a triplicate of intensity profiles for a given condition, a single expression value for each probe set. Following that step the ratio experiment pipeline from Resolver was used to obtain *n*-fold changes between treatment versus time-matched untreated intensity experiments. A probe set with intensity *P* values given by the Affymetrix error model from Resolver below 10^{-6} was considered present. *n*-Fold changes in *P* significance values for probe sets were derived from Resolver using a two-sample *t* test with no false discovery rate correction. Moreover, a principal component analysis (PCA) was performed using the intensities profiles obtained for the untreated, dexamethasone, retinoic acid, and PD174265 samples at each time point (10, 24, and 72 h). Only probe sets called present in at least three arrays and with a variation coefficient greater than 0.3 were kept in the PCA step.

A two-dimensional agglomerative Resolver HCA procedure using z-score-transformed intensity experiments with a cosine correlation similarity measure and the Ward's minimum variance heuristic criteria was applied on two probe sets selections for untreated, dexamethasone, retinoic acid, and PD174265 conditions at 10 and 72 h.

The first probe set selection used in the HCA corresponds to the genes listed in Tables 1 and 2.

To generate the second probe set list, *n*-fold changes comparing each treatment and time point versus the respective time-matched untreated samples for dexamethasone, retinoic acid, and PD174265 were examined, and 4,268 probe sets with an absolute change value of >2-fold, a corresponding *P* value of <0.01, and an intensity experiment value >50 in either treated or untreated condition at any time point were selected.

Western blot. Sodium dodecyl sulfate-polyacrylamide gels (Invitrogen NuPAGE Novex Bis-Tris gels,12%) were run according to the manufacturer's instructions, and proteins were transferred to nitrocellulose membrane (Invitrogen LC2001) using a semidry transfer apparatus (Hoefer SemiPhor; Amersham Pharmacia Biotech). The membrane was blocked in washing buffer (phosphate-buffered saline [PBS], 0.2% Tween 20) plus 5% dissolved nonfat milk powder. It was incubated overnight at 4°C with anti-CNP (M-300) Santa Cruz sc-30158 rabbit polyclonal antibody or anti-MBP (C-16) Santa Cruz sc-13914 goat polyclonal antibody at a 1:1,000 dilution. The blot was washed, incubated for 1 h at room temperature with a corresponding horseradish peroxidase (HRP)-conjugated antiserum (goat anti-rabbit Ig-HRP [Bio-Rad 170-6515] or donkey anti-goat Ig-HRP [Santa Cruz sc-2020] at 1:2,000 dilution), washed again, and visualized by chemiluminescence (ECL kit; Amersham Pharmacia Biotech RPN 2106).

CNP enzymatic assay. siRNA-transfected cells in 96-well plate were lysed, after 3 days (~80% confluence), in 80 μl of triple-detergent buffer (50 mM Tris [pH 8], 150 mM NaCl, 0.1% sodium dodecyl sulfate, 1% NP-40, 0.5% sodium deoxycholate) with complete protease inhibitor cocktail (Roche catalog no. 11836170001) and then incubated for 15 min at room temperature. The protein content was measured using a BCA protein assay kit (Pierce catalog no. 23225). Then, 2.5 μg of total protein was plated in a black Costar 96-well plate, and the cyclic nucleotide phosphodiesterase (CNP) reaction was run in 100 μl of 200 mM MES free acid hydrate (Sigma M8250)–30 mM $MgCl_2$–1.11 mM 2′-3′-cNADP (Sigma N5257)–5.55 mM glucose-6-phosphate (Sigma G7879)–0.06 U of glucose-6-phosphate-dehydrogenase (Sigma G8164) for 15 min at room temperature. The fluorescence intensity (FI) was read on a Perkin-Elmer Victor 2 spectrofluorimeter (excitation at 355 nm, emission at 460 nm, for 0.1 s) and normalized for protein content.

Cellomics readout using O4 staining. siRNA-transfected cells in 96-well plates were fixed with 4% paraformaldehyde 15 min at room temperature, washed twice with 1× PBS, and incubated with 50 μl per well of mouse anti-O4 monoclonal antibody diluted 20 times in 1× PBS at 4°C overnight. Cells were washed twice with 1× PBS and incubated with 50 μl per well of anti-mouse immunoglobulin M-Alexa Fluor 488 (Invitrogen A21042) diluted 200 times and incubated for 1 h at room temperature. Nuclei were stained with Hoechst dye diluted 10,000-fold for a further 15 min. Cells were washed twice with 1× PBS before fluorescent cell images were obtained on an ArrayScan HCS reader with a ×5 or ×10 objective lens, and effective image analysis was done by Cellomics Technologies (Thermo Scientific) for determination of the "neurite outgrowth" (NOG) index.

MBP enzyme-linked immunosorbent assay (ELISA). siRNA-transfected cells in 96-well plate were fixed with 1% glutaraldehyde (Fluka catalog no. 49631) in 1× PBS for 15 min room temperature, washed twice with 1× PBS, and incubated

TABLE 1. "Core" differentiation genes selected for functional analysis[a]

HUGO name	Affmetrix probeset	RefSeq no.	10 h		24 h		72 h	
			Dex	PD	Dex	PD	Dex	PD
Abat	1433855_at	NM_172961	3.1	3.8	2.6	3.7	2.5	2.8
Abca1	1450392_at	NM_013454	2.8	3.5	2.2	1.6	1.6	-1.1
Ankrd6	1421386_at	NM_080471	2.4	3.4	-1.9	1.2	-2.0	-1.1
App	1444705_at	NM_007471	-2.5	-4.2	-1.7	-1.6	-1.4	-1.3
Aqp11	1455411_at	NM_175105	4.9	4.3	-1.0	1.0	3.5	3.7
Atrn	1421166_at	NM_009730	2.1	3.4	1.4	2.2	1.2	2.0
Bcas3	1423528_at	NM_138681	2.0	2.6	1.7	1.7	1.1	1.0
Brwd3	1441182_at	XM_987351	3.1	3.5	1.4	1.2	-1.8	-1.6
C230027C17	1435612_at	NM_177906	3.0	4.5	-1.2	-1.0	-2.0	-1.4
Ccng1	1450016_at	NM_009831	2.2	2.6	1.5	1.6	1.4	1.1
Cdk6	1435338_at	NM_009873	-4.2	-5.5	-5.0	-5.8	-7.2	-4.8
Ddah1	1438879_at	NM_026993	-2.5	-3.4	-1.1	-1.6	-1.1	-1.1
Dixdc1	1443957_at	NM_178118	2.0	3.9	1.3	2.3	1.1	1.8
Dscaml1	1432196_a_at	XM_991821	2.7	3.6	1.5	2.5	1.9	3.7
E2f1	1417878_at	NM_007891	-2.9	-3.3	-3.7	-4.0	-1.8	-1.5
Elmo1	1450208_a_at	NM_080288	30.2	4.2	29.0	6.1	14.6	2.1
Enpp6	1442075_at	ND	3.6	7.9	-1.2	53.3	1.4	79.2
Ext1	1458054_at	NM_010162	-2.6	-3.1	-1.3	1.0	-1.0	1.1
Hbp1	1432143_a_at	NM_177993	3.3	5.8	1.8	2.1	1.2	1.4
Ikbke	1417813_at	NM_019777	2.6	3.5	1.1	2.2	1.8	1.4
Il6ra	1452416_at	NM_010559	3.7	2.5	2.3	-1.0	2.1	1.6
Kcna1	1417416_at	NM_010595	6.0	7.8	18.2	29.5	16.4	35.5
Lrrn1	1416053_at	NM_008516	2.5	10.1	1.1	7.1	-1.1	5.2
Ly78	1446165_at	NM_008533	-2.9	-4.2	1.1	-1.0	1.2	1.3
Mamdc1	1442561_at	NM_207010	-2.4	-3.1	-1.2	-1.3	-1.5	-1.4
Mbp	1451961_a_at	NM_010777	2.4	2.8	2.0	2.6	2.0	2.3
Mtap7	1421835_at	NM_008635	9.8	2.2	11.7	5.0	14.1	5.7
Narf	1425344_at	NM_026272	2.9	4.9	1.4	2.4	1.5	1.8
Ndrl	1420760_s_at	NM_008681	4.6	14.8	5.8	5.4	13.4	7.8
Numb	1425368_a_at	NM_010949	3.3	3.6	1.3	2.3	-1.4	1.1
Oas1g	1424775_at	NM_145211	4.0	6.4	1.5	-1.2	-1.1	-1.6
Pak3	1417924_at	NM_008778	2.3	4.1	-1.3	1.7	-1.2	1.7
Pak7	1440981_at	NM_172858	3.7	5.7	5.6	9.2	2.9	6.2
Pps	1456412_a_at	NM_008916	2.1	3.7	1.9	2.5	1.8	2.0
Ptdss2	1453164_a_at	NM_013782	3.3	4.4	1.1	1.2	2.1	1.6
Rab2b	1455857_a_at	NM_172601	2.1	2.6	1.3	1.8	1.6	2.1
Rgs2	1419247_at	NM_009061	4.3	2.8	5.9	2.5	5.7	1.8
Rnf13	1420620_a_at	NM_011883	2.5	3.7	1.2	1.5	1.1	1.0
Rpgrip1	1458526_at	ND	-2.6	-2.7	1.1	-1.6	-1.3	-1.2
Slc25a27	1454230_a_at	NM_028711	4.2	5.6	3.3	3.3	2.6	1.5
Sorbs1	1417358_s_at	NM_009166	2.4	3.6	1.5	1.1	1.2	1.5
Tal2	1450517_at	NM_009317	2.7	2.8	-1.0	-1.5	-1.5	-1.6
Tnc	1416342_at	NM_011607	-2.9	-4.8	-3.8	-8.7	-3.0	-6.5
Tnni1	1450813_a_at	NM_021467	2.4	2.9	3.3	2.0	12.9	7.4
Trp53inp1	1416927_at	NM_021897	7.8	7.6	2.1	1.9	1.1	-1.5
Ugt8a	1419064_a_at	NM_011674	2.1	4.0	1.5	4.6	1.3	3.9
Zfpn1a5	1436554_at	NM_175115	2.2	2.3	1.1	1.5	1.1	1.5
Zkscan1	1453051_at	NM_133906	2.4	3.1	1.8	3.0	1.4	1.7

[a] The Affymetrix probe set codes and expression changes in Oli-neu induced for differentiation by dexamethasone (Dex) or PD174265 (PD) are indicated by colors as follows: yellow, 1.5- to 2-fold induction; orange, 2- to 4-fold induction; red, >4-fold induction. Dark green indicates a 1.5- to 2-fold reduction; bright green indicates a >2-fold reduction.

TABLE 2. Additional genes selected for knockdown analysis (see the text)[a]

HUGO name	Affmetrix probeset	RefSeq no.	10 h		24 h		72 h	
			Dex	PD	Dex	PD	Dex	PD
Cd81	1416330_at	NM_133655	1.3	1.4	1.8	2.5	1.7	2.1
Erbb2ip	1428011_a_at	NM_021563	1.3	1.6	1.4	2.0	1.7	2.2
Fyn	1448765_at	NM_008054	1.1	1.1	1.4	2.3	1.1	1.3
Grid2	1435487_at	NM_008167	-1.1	-1.0	1.6	2.1	1.1	-1.1
Grik2	1425790_a_at	NM_010349	2.1	3.9	1.6	2.5	-1.1	1.3
Itpr1	1417279_at	NM_010585	1.6	-2.2	1.5	-3.9	1.2	-7.6
Kit	1452514_a_at	NM_021099	-1.1	-2.6	1.3	-2.4	1.4	-5.2
Nlgn3	1436135_at	NM_172932	-1.6	-1.0	1.2	3.0	1.6	1.9
Pik3r1	1425515_at	NM_011085	2.4	-1.1	2.0	-1.3	1.7	-2.1
Plcb1	1435043_at	NM_019677	2.2	1.4	2.5	2.6	1.8	1.1
Ptprr	1426047_a_at	NM_011217	2.0	1.1	2.9	1.4	1.3	-1.2
Reln	1449465_at	NM_011261	-1.0	1.5	-1.0	3.5	2.2	9.0
Tal1	1449389_at	NM_011527	-2.0	-2.7	-1.9	-2.8	-1.7	-2.0
Tgn	1450790_at	NM_009375	-1.1	1.2	-1.1	1.3	1.2	5.9
Trpc4	1451033_a_at	NM_016984	2.3	2.3	3.8	2.0	3.2	1.3
Tspan2	1424567_at	NM_027533	1.1	2.7	1.1	4.5	-1.0	4.0
Clic5	1456873_at	NM_172621	-2.1	-5.8	-3.0	-14.0	-2.6	-21.7
Cnp1	1449296_a_at	NM_009923	1.4	2.4	2.0	4.7	2.4	4.5
Creb5	1442576_at	NM_172728	-1.9	-3.0	-1.6	-3.8	1.1	-1.6
Dab1	1427307_a_at	NM_010014	-1.5	-2.4	-1.7	-2.8	-1.9	-2.9
Dusp10	1417164_at	NM_022019	1.3	4.5	2.9	5.9	3.4	8.7
Dusp4	1428834_at	NM_176933	-2.8	-17.3	-2.8	-15.8	-3.6	-36.3
Dusp6	1415834_at	NM_026268	1.2	-11.1	1.2	-6.5	1.1	-9.7
Egr1	1417065_at	NM_007913	-1.3	-12.5	-1.3	-13.1	1.0	-10.2
Etv4	1423232_at	NM_008815	-1.6	-16.1	-1.8	-100.0	-1.8	-86.6
F3	1417408_at	NM_010171	2.6	-5.0	2.9	-5.3	2.3	-4.4
Hbp1	1432143_a_at	NM_153198	3.3	5.8	1.8	2.1	1.2	1.4
Klhl2	1458351_s_at	NM_178633	1.2	1.6	2.0	4.5	1.9	4.0
Map2k4	1451982_at	NM_009157	1.1	1.6	1.6	2.0	1.1	1.5
Map4k5	1427084_a_at	NM_024275	1.3	2.4	1.3	3.7	1.1	3.5
Pak1	1450070_s_at	NM_011035	1.5	2.3	2.0	4.2	3.8	5.0
Plp1	1425467_a_at	NM_011123	1.6	2.1	2.2	5.3	2.6	4.6
Pou3f1	1422068_at	NM_011141	-1.1	-30.4	-1.3	-58.2	-1.6	-71.6
Ptpn9	1451037_at	NM_019651	-1.3	-2.8	-1.2	-1.7	-1.2	-1.6
Ptpre	1418539_a_at	NM_011212	-1.2	2.0	1.4	4.5	-1.4	1.7
Ptprj	1455030_at	NM_008982	1.6	-1.2	2.4	2.1	1.9	1.9
Ptpro	1417676_a_at	NM_011216	-1.3	1.2	1.3	2.6	-1.2	1.0
Shc4	1457118_at	NM_199022	-1.3	-3.0	1.1	-2.7	-1.1	-4.4
Sirt2	1423507_a_at	NM_022432	1.5	3.0	2.0	11.7	1.8	7.0
Spry4	1440867_at	NM_011898	-1.3	-18.9	-1.4	-25.1	-1.3	-17.8

[a] Color shading is as defined in Table 1, footnote *a*.

1 h at room temperature in blocking buffer (PBS, 0.2% Tween 20, 5% nonfat milk powder). Cells were incubated with anti-MBP (C-16; Santa-Cruz sc-13914) goat polyclonal antibody at a 1:400 dilution in 5% milk–TBS (Tris-borate-EDTA)–0.1% Tween 20 overnight 4°C. After two washes in 1× PBS–0.2% Tween, cells were incubated with donkey anti-goat Ig-HRP (Santa Cruz sc-2020) antibody at a 1:400 dilution in 5% milk–TBS–0.1% Tween 20 for 1 h at room temperature. Cells were washed twice in 1× PBS–0.2% Tween and once in 1× PBS before we assessed the HRP activity with its chromogenic substrate ABTS [2,2′azinobis(3-ethylbenzthiazolinesulfonic acid); Sigma A1888] and obtained a reading at 405 nm.

Phosphatase assays. Unless otherwise stated, chemicals were purchased from Sigma-Fluka (Saint-Louis, MO). DiFMUP (6,8-difluoro-4-methyumbelliferyl phosphate) was obtained from Molecular Probes/Invitrogen (Carlsbad, CA). N-terminally fluorescein-labeled (Fl) phosphopeptide [EAIY(PO3)AAPFA] was purchased from Caliper Life Sciences (Hopkinton, MA). The 96- and 384-well plates were from Corning Inc. (Corning, NY). The glutathione *S*-transferase-tagged catalytic domain of the human phosphatases MKP5, PAC1, PTP1B, PTPβ, PTP-H1, PTPμ, SHP1, SHP2, TC-PTP, VHR, and Glepp1 were cloned, expressed in *Escherichia coli*, and purified by affinity analysis on a glutathione column as described previously (32, 41).

Mobility shift assay for MKP5 inhibitors. Assays were performed in 384-well plates. A total of 5 μl of fluorescein-labeled peptide substrate at 3 μM in reaction buffer (20 mM Bis-Tris-HCl [pH 6.2], 0.01% Igepal, 5 mM dimethyl sulfoxide [DMSO]), corresponding to a 1 μM peptide final concentration, was added to 5-μl portions of compounds in 5% DMSO. The reaction was started by the addition of 5 μl of the enzyme at a concentration of 0.66 μg/ml (corresponding to a final concentration of 0.22 μg/ml) in reaction buffer containing 3 mM DL-dithiothreitol. After 2 h of incubation, 15 μl of termination buffer (100 mM HEPES [pH 7.5], 0.01% Igepal, 0.1% coating reagent 3, 5% DMSO) was added. Aliquots from each well were sipped by a 12 sippers chip model 760137-0372R on a HTS 250 drug discovery system instrument (Caliper Life Sciences) for electrophoretic separation of the substrate and product peaks and measurement of the FI of the peaks (1). The relative peak heights of the substrate and product were measured, and ratios were calculated using HTS Well Analyzer Software 4.1 from the manufacturer. The ratio (r) was defined as the height of the product peak divided by the sum of the peak height of the product and substrate. The low controls corresponded to the absence of enzyme in columns 1 and 2 (A-H) and 24, and the high controls corresponded to the absence of compounds in columns 1 and 2 (I-P). The percent inhibition was calculated relative to the high and low controls as $100 \times [1 - (r - r_{\text{low control}}/r_{\text{high control}} - r_{\text{low control}})]$.

DiFMUP-based assay for phosphatase selectivity. For selectivity phosphatase assays were carried out using a DiFMUP concentration corresponding to the K_m of the enzyme studied (2). In 96-well plates containing 5 μl of diluted compound or solvent (100% DMSO) in each well, 55 μl of DiFMUP diluted in PTP buffer (20 mM Bis-Tris-HCl [pH 7.5], 0.1% Brij 35, 1 mM DL-dithiothreitol) was added, followed by 40 μl of recombinant enzyme diluted in PTPB buffer in order to start the reaction. After 45 min at room temperature, the FI was measured (excitation at 355 nm and emission at 460 nm for 0.2 s) on a Perkin-Elmer Fusion spectrofluorimeter (Perkin-Elmer Life Sciences). Negative controls were performed in the absence of enzyme, and positive controls were carried out in the presence of enzyme without compound. The percentage of activity was calculated according to the following formula: $\%\ \text{activity} = 100 \times (\text{FI}_{\text{compound}} - \text{FI}_{\text{low control}})/(\text{FI}_{\text{high control}} - \text{FI}_{\text{low control}})$. The 50% inhibitory doses (IC_{50}) were determined in triplicate in two independent experiments.

Gene Expression Omnibus database accession number. The expression data described here have been deposited in the NCBI Gene Expression Omnibus database (http://www.ncbi.nlm.nih.gov/geo) under accession number GSE14406.

RESULTS

Genes regulated during OPC (Oli-neu) differentiation. Full oligodendrocyte differentiation involves process formation, followed by myelin production (see, for example, reference 30). In earlier work, we used the OPC Oli-neu cell line (18) to discover new differentiating agents, using as readout an automated (Cellomics) protocol that measured oligodendrocytic process formation with O4 monoclonal antibody (36) immunostaining (unpublished data). Screening pharmacologically active compounds from the LOPAC (Sigma-Aldrich) and National Institute of Neurological Disorders and Stroke libraries, we discovered three active compound classes, represented in the present study by forskolin (which activates adenylyl cyclase, cyclic AMP synthesis, and protein kinase A), retinoic acid and dexamethasone (both steroid hormones), and PD174265 (an ErbB-family kinase inhibitor). As schematically shown in Fig. 1 (left panel), treatment of cells with these agents at their optimal dose induced differentiation to various extents: while all compounds induced process formation (shown for PD174265 at the bottom of the figure), forskolin induced only partial ramification and trace MBP production, whereas the steroids and PD174265 also induced increasing amounts of MBP (measured by using Western blots). Differentiation of Oli-neu cells for all treatments was accompanied by induction of CNP, PLP-1, O4 signal, and other markers previously described for primary OPCs as well (9), indicating that these agents are bona fide inducers of differentiation (data not shown).

Our experimental setup for genome-wide expression analysis is outlined in Fig. 1 (right panel). Once stable experimental conditions were established, Oli-neu cell differentiation was induced by using the four active treatments, with insulin and untreated cells as controls. RNA was isolated at the 0 (shared)-, 10-, 24-, and 72-h time points. These time points were based on pilot time course experiments wherein we examined cell morphology and markers. Three biological replicates (separate cultures) were taken for each time-treatment combination and, after RNA isolation, quality control, and cRNA synthesis, each replicate was individually hybridized to a microarray (see Materials and Methods). The resulting data set was analyzed for overall quality by PCA (Fig. 2A). PCA is used to analyze complex exploratory datasets in which each measurement (in this case, gene expression change) is associated with multiple "coordinates," in our case (i) treatment, (ii) time point, and (iii) biological replicate. This multivariate analysis then attempts to reveal an internal structure in the data set, specifically to determine to what extent each "coordinate" is responsible for data variation. The analysis showed that biological replicates clustered closely, indicating good experimental reproducibility, and that the nature of treatment was the strongest driver of principal component 1 (horizontal axis) with duration of treatment (time) driving component 2 (vertical axis). Since the forskolin treatment clustered closely with the untreated set, it was left out of Fig. 2A. This plot also demonstrates that PD174265 treatment differed from treatment with the steroids in that transcriptional changes appeared already final at 24 h (proximity of 24- and 72-h clusters), unlike the other treatments.

We next subjected the 10- and 72-h time point intensity data to unsupervised HCA, as shown in Fig. 2B. This analysis demonstrated significantly better clustering between the two PD174265 time points than between PD174265 and any of the steroids. Cluster 3 comprises mostly genes whose low expression (relative to controls) associated with differentiation, whereas the genes in cluster 5 were strongly upregulated by PD174265, particularly at later stages of differentiation. Further analysis of the genes in these clusters (listed in the supplemental material) using Ingenuity Pathway Software analysis indicated that Cluster 3 is enriched for genes associated with axonal guidance signaling and nervous system development, whereas cluster 5 genes associated with cell cycle progression and proliferation (a full analysis shown in the supplemental

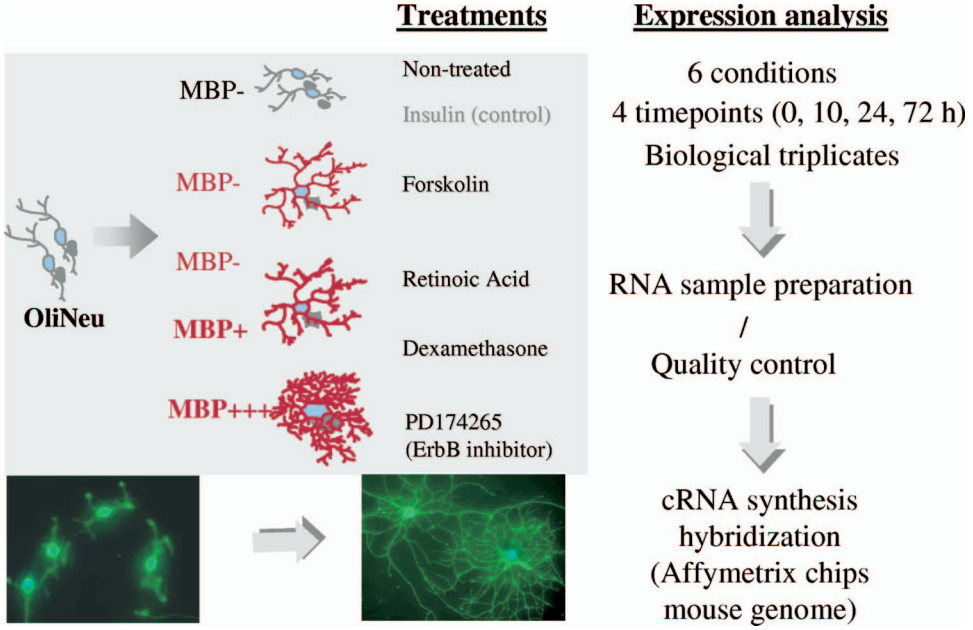

FIG. 1. Experimental setup of gene expression analysis. (Left) Oli-neu cells were induced by using four different chemical treatments (forskolin, retinoic acid, dexamethasone, and PD174265) compared to untreated or insulin-treated controls. Differentiation results in variable synthesis of MBP and dendrocyte outgrowth, measured using O4-stained immunofluorescence (for PD174265; shown at the bottom). (Right) Chip hybridization protocol. Each whole-genome Affymetrix chip was hybridized to one of three biological triplicate of cell cultures from six treatments over four time points (61 hybridizations; $t = 0$ shared).

material). In Ingenuity Pathway analysis, genes in a given cluster (e.g., showing similar transcriptional behavior) are electronically mapped to networks built from published gene-gene interactions as retrieved from the (full-text) biomedical literature. The curated network database that we consulted for the present study contained data from human and rodents. Networks retrieved using this method are ranked by the number of "hits" from the query gene set.

Overall, these analyses indicated that different treatments affected different gene sets, even though they induced a similar phenotype. We counted regulated genes common for multiple treatments for various time points using Venn diagrams (Fig. 3A to E; see Materials and Methods for data analysis). Genes in overlaps were counted, while including forskolin (Fig. 3A and D) or insulin (control; Fig. 3C to E) or including only a single steroid treatment (Fig. 3C and D). Counting only genes associated with differentiation (red intersections, listed numbers) showed a clear, time-dependent increase for all diagrams. This trend was not seen for the totals of modulated genes for each treatment (Fig. 3F), thus demonstrating true convergence of the phenotype with a specific, complex transcriptional signature. We conclude that the oligodendrocyte differentiation process is characterized by an expanding set of commonly modulated genes, while individual treatments produce additional, likely unrelated transcriptional "noise." However, we cannot exclude that this "noise" represents in fact alternative, inducer-specific paths toward the differentiated state. We reasoned that the shared gene sets (Venn diagram intersections) might be enriched for key players in the differentiation process.

For further (functional) analysis, we focused on genes represented in the red intersection in Fig. 3E. For this overlap we considered early (10-h) genes modulated significantly ($P <$ 0.01) ≥2-fold by PD174256 and >2-fold and >1.5-fold by dexamethasone and retinoic acid, respectively. The reason for looking at the early 10-h time point is that this is the "process-forming" differentiation stage induced by all treatments (Fig. 1); thus, this time point reflects true phenotypic convergence. The 48 genes in this overlap are listed in Table 1, with expression changes indicated for dexamethasone and PD174265 for the three time points.

Functional involvement of genes whose activity is modulated through differentiation regardless of induction mode. Having identified a set of "signature" genes whose expression changes specifically accompany Oli-neu differentiation as induced by various agents, we next sought to understand which of these genes are functionally involved in the process, using siRNA-mediated gene silencing. In addition to the genes listed in Table 1, we also included two other sets of genes that were regulated during differentiation but did not fulfill all inclusion criteria. Such genes were included (Table 2, upper panel) because they also have chromosomal single-nucleotide polymorphisms that were statistically associated with multiple sclerosis (H. Abderrahim, unpublished data). We also included additional, regulated genes (Table 2, lower panel) from mitogen-activated protein kinase (MAPK) signaling pathways and associated dual-specificity phosphatases (DUSPs) and oligodendrocyte-specific genes as reported in the literature.

For functional interrogation of the gene set listed in Tables 1 and 2, we considered two experimental approaches. The first sought to determine which genes are essential for differentiation. This was attempted by treating Oli-neus with siRNAs, followed by treatment with the chemical inducers. Unfortunately, we failed to identify such gene candidates with confidence; since only a percentage of cells is RNAi transfected and

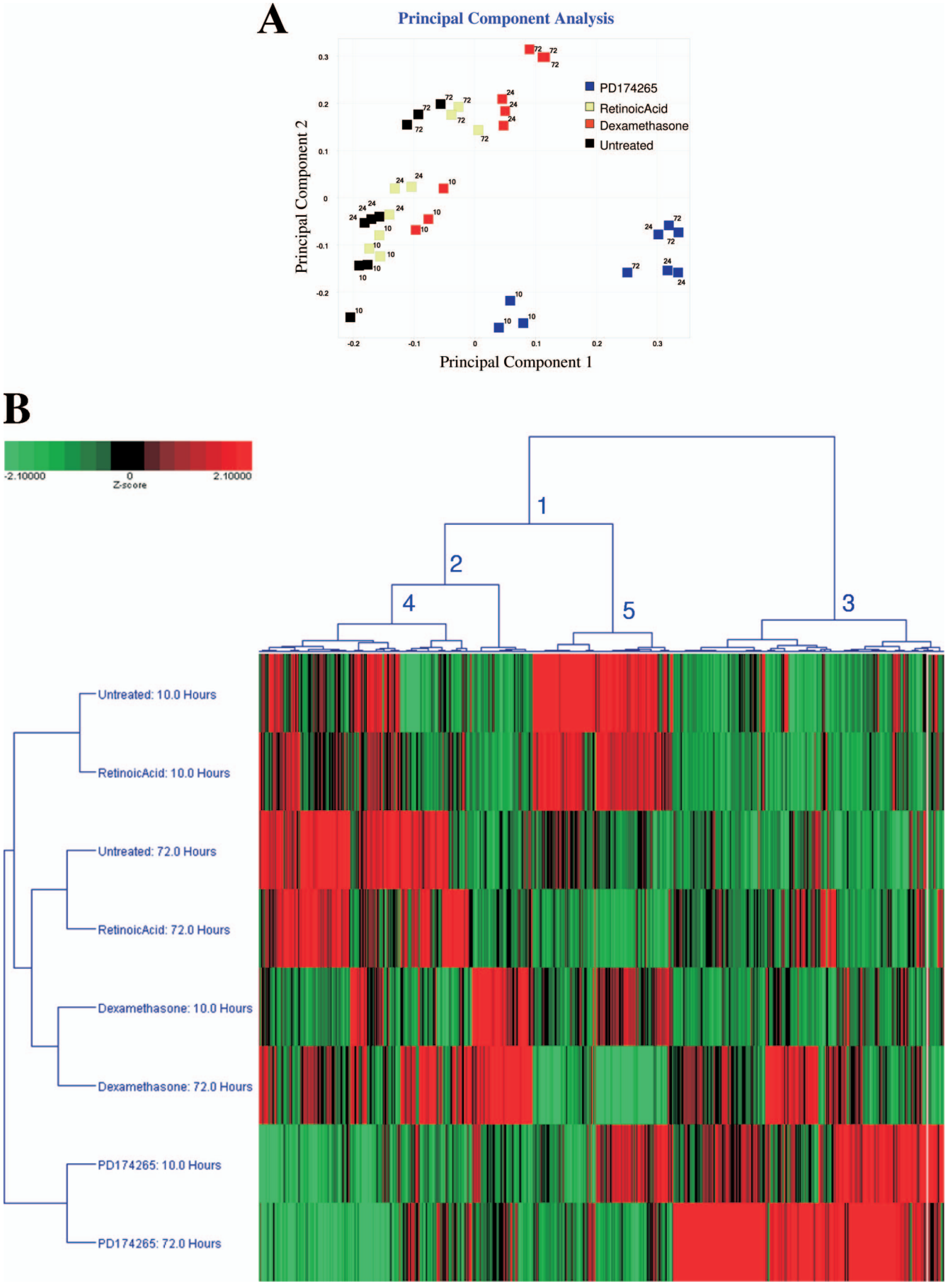
A
Principal Component Analysis
PD174265
RetinoicAcid
Dexamethasone
Untreated
Principal Component 2
Principal Component 1
B
-2.10000
0
2.10000
Z-score
1
2
3
4
5
Untreated: 10.0 Hours
RetinoicAcid: 10.0 Hours
Untreated: 72.0 Hours
RetinoicAcid: 72.0 Hours
Dexamethasone: 10.0 Hours
Dexamethasone: 72.0 Hours
PD174265: 10.0 Hours
PD174265: 72.0 Hours

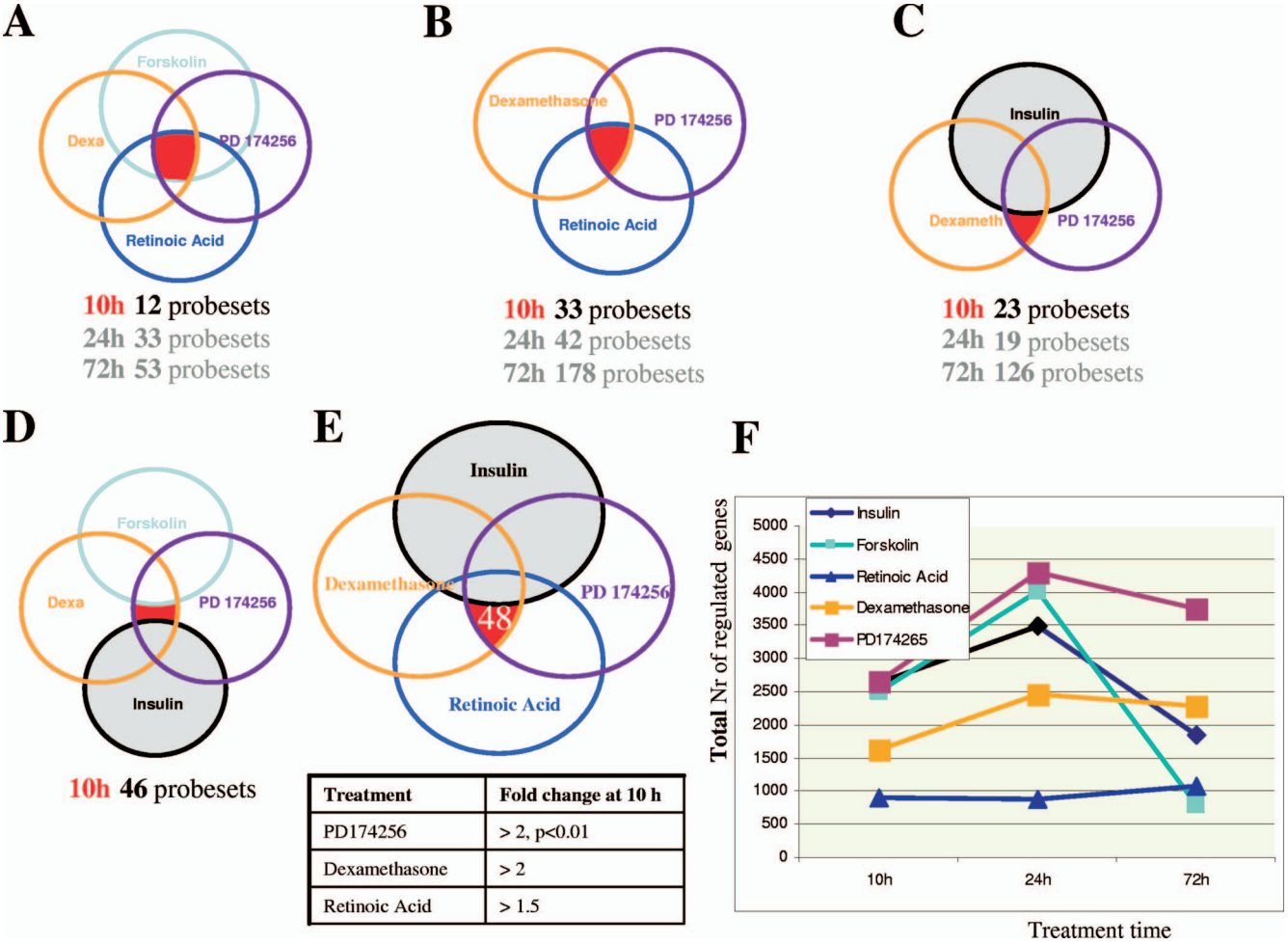

Treatment	Fold change at 10 h
PD174256	> 2, p<0.01
Dexamethasone	> 2
Retinoic Acid	> 1.5

FIG. 3. Genes specifically regulated by various differentiating agents. (A to D) Number of genes (probesets) significantly up- or downregulated (>2-fold, compared to untreated cells at the same time point) common to various combination of treatments. The numbers below each Venn diagram refer to the red-colored overlapping section and are given for different time points. (E) Overlap and criteria for the set of 48 genes selected for functional analysis (see also Table 1 and the text). (F) Total numbers of genes modulated (>2-fold) per treatment at different time points.

yet all respond to the inducing chemical, our positive controls failed (I. Foucault, unpublished data). We then looked for genes whose silencing might drive spontaneous differentiation. The readout in this protocol (see below) is quite sensitive, and this approach did produce a number of potential positives.

For each of the 88 selected genes (Tables 1 and 2), two siRNAs were tested, targeting exons found in each (or in a majority of) transcripts for a given gene (all siRNAs and their sequences are given in the supplemental material). In the initial step of our screening procedure, Oli-neus were transfected in duplicate (for each siRNA) in 96-well plates, and after 72 h the lysates were tested for CNP activity. A surprisingly large subset of 47 siRNAs showed activity, and these were retested in six-well plates using CNP, MBP, and PLP qPCR analysis as readouts (data not shown). Finally, for 16 genes that were selected from this set, both siRNAs (for each gene) were tested in a 12- or 24-well format. Differentiation was measured by CNP enzymatic activity (Fig. 4A); MBP ELISA (Fig. 4B); qPCR analysis for PLP (Fig. 4C), MBP (Fig. 4D), or CNP mRNA (Fig. 4E); and in a 96-well format with Cellomics readout using O4 monoclonal antibody staining for process formation (Fig. 4F). Induction of differentiation was compared to luciferase siRNA (negative control). As a positive control, we used siRNA for ErbB2 (Neu), the target of the PD174265 inhibitor in these cells. As shown in Fig. 4, a number of siRNAs induced

FIG. 2. (A) Intensity profile PCA for untreated, retinoic acid, dexamethasone, and PD174265 induced gene expression data. The numbers indicate time points (in hours). (B) HCA for 4,260 probe set expression values at 10 and 72 h for untreated, dexamethasone, retinoic acid, and PD174265 conditions. Five clusters were defined; clusters 3 (1,695 probe sets) and 5 (875 probe sets) were retained for further analysis (listed and analyzed in in the supplemental material).

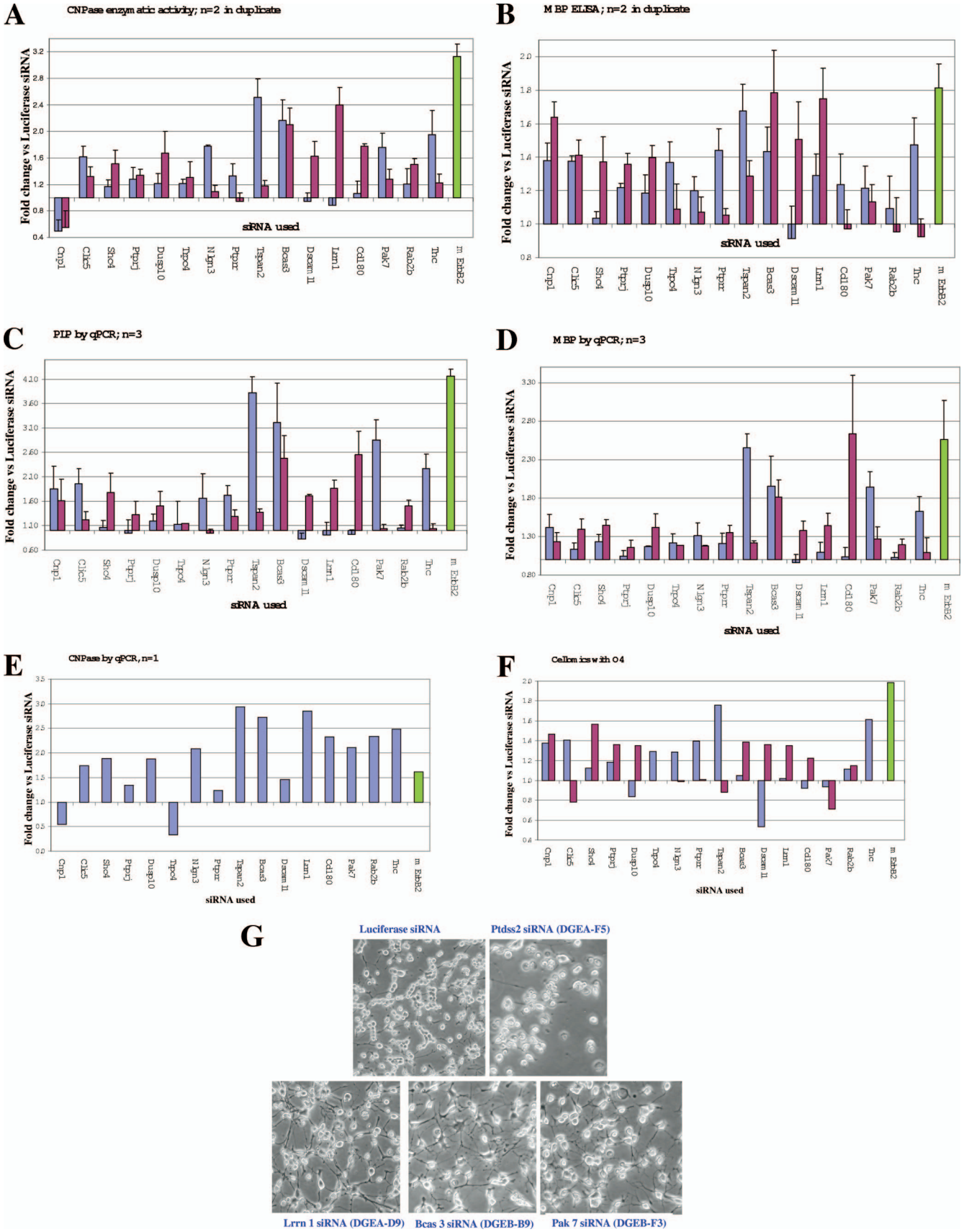
A
CNPase enzymatic activity; n=2 in duplicate
Fold change vs Luciferase siRNA
siRNA used
Cnp1
Clic5
Shc4
Ptprj
Dusp10
Tpc4
Nlgn3
Ptpnr
Tspan2
Bcas3
Dscam l1
Lrrn1
Cd180
Pak7
Rab2b
Thc
m ErbB2
B
MBP ELISA; n=2 in duplicate
Fold change vs Luciferase siRNA
siRNA used
C
PIP by qPCR; n=3
Fold change vs Luciferase siRNA
siRNA used
D
MBP by qPCR; n=3
Fold change vs Luciferase siRNA
siRNA used
E
CNPase by qPCR, n=1
Fold change vs Luciferase siRNA
siRNA used
F
Cellomics with O4
Fold change vs Luciferase siRNA
siRNA used
G
Luciferase siRNA
Ptdss2 siRNA (DGEA-F5)
Lrrn 1 siRNA (DGEA-D9)
Bcas 3 siRNA (DGEB-B9)
Pak 7 siRNA (DGEB-F3)

differentiation, as judged by mRNA and protein expression of markers. In contrast, Dscaml1 (named for Down syndrome cell adhesion molecule-like 1) produced inconsistent results (with only one siRNA being active and the other showing opposite behavior). A notable and unexpected "positive" is CNP/CNP1; while its siRNAs reduced expression of CNP protein and mRNA (Fig. 4A and E, leftmost bars); this silencing was accompanied by Oli-neu differentiation induction, as seen for all other tested markers (Fig. 4B, C, D, and F). Induction of differentiation markers was accompanied by changes in microscopic morphology (process formation), as shown for selected genes in Fig. 4G. The lower panel in this figure represents active siRNAs; the top panel shows negative siRNAs.

Evaluation of differentiation inducer genes in primary oligodendrocytes. In order to further validate our results, we decided to examine the set of active genes in primary OPCs from newborn rat. After isolation, OPCs were transfected with rat siRNAs for 10 of the most active genes identified earlier in Oli-neu cells, and differentiation was followed by monitoring mRNA expression (qPCR) for MBP and proteolipid protein 1 (Fig. 5A) and for CNP and MBP protein using Western blot analysis (Fig. 5B). Like for Oli-neu, luciferase siRNA was used as negative control and (rat) ErbB2 siRNA was used as a positive control to induce differentiation. No rat siRNAs could be obtained for Shc4 and Tnc (tenascin C), while OPC expression of Clic5 (chloride intracellular channel 5), Bcas3 (breast carcinoma amplified sequence 3), and Cd180 was too weak to pursue these genes. As shown in Fig. 5A, the majority of test genes induced differentiation in these primary precursors as well. However, no convincing activity was found for Pak7 (p21 protein activated kinase 7) and Lrrn1 (leucine-rich neuronal protein 1), using siRNAs that repressed their cognate mRNA levels by 66 and 57%, respectively (bulk silencing efficiencies are indicated in Fig. 5A, bottom). Dscam1 again produced inconclusive results, possibly related to low overall silencing efficacy (48%) of its siRNA. In contrast, we confirmed for the other seven genes that their repression results in spontaneous differentiation in OPCs, as shown earlier for Oli-neu cells. We also confirmed that silencing of CNP, 78% by qPCR (Fig. 5A) and confirmed by Western blotting (Fig. 5B), resulted in induction of proteolipid protein 1 mRNA and MBP mRNA and protein.

In an attempt to determine how these seven gene products interact and induce differentiation with PLP and MBP synthesis, we assessed their fit into a network of literature-based, direct gene-to-gene interactions, using Ingenuity Pathway Analysis software. As shown in Fig. 6, all genes submitted to this analysis (indicated in yellow) could be fit into a single set of linked pathways, annotated as involved in neurological disease/cell morphology. This view is centered on a MAPK signaling cascade involving MAPK3 (Erk1) and MAPK1 (Erk2) driving expression of MBP and PLP. The three PTPs (DUSP10/MKP5, PTPRR/PTPSL/PCPTP1, and PTPRJ/DEP/PTPη) are all known to exert negative control on this cascade, while Nlgn3 (neuroligin 3) and Trpc4 (transient receptor potential cation channel 4) may enter the system via Src and Dlg4/PSD-95, the latter being a central nervous system-restricted guanylate kinase.

Induction of oligodendrocyte differentiation using a novel MKP5 inhibitor. The identification of genes whose repression results in spontaneous OPC differentiation may lead to the discovery of drugs that promote remyelination in patients suffering from multiple sclerosis or other myelin-related disorders. Among the genes that we identified, PTPRJ, PTPRR, DUSP10/MKP5 and CNP1 are, in principle, "druggable" enzymes. Among these, MKP5 is of special interest, since earlier work has shown that mice that lack this gene are significantly protected from experimental autoallergic encephalitis (45). We found that knockdown of MKP5 results in significant induction of OPC differentiation (Fig. 7A). We have used a novel, organic inhibitor of Dusp10/MKP5, AS077234-4, which inhibited MKP5 in vitro with an IC_{50} of 710 nM, displayed selectivity among protein tyrosine phosphatases (Fig. 7B), and showed no inhibition in a large, general panel of G-protein-coupled receptors (data not shown). As shown in Fig. 7C and D, treatment of rat OPCs with this inhibitor, starting at 0.3 to 1 μM, induced MBP and CNP protein production. This result suggests that inhibition of MKP5 catalytic activity (like RNAi-mediated mRNA degradation) is sufficient to promote OPC differentiation, validating MKP5 as a potential target for diseases where enhanced OPC differentiation has therapeutic value.

Kinetics of differentiation-associated gene expression. Earlier differential gene expression work on rat OPCs had characterized "early" and "late" waves of induced genes (9). We analyzed these groups of genes (their mouse orthologs) in our data set. Among the earlier described genes, Osp/claudin11 and Tm4sf11/plasmolipin were not found on the mouse genome chips, while Mobp (myelin-associated oligodendrocyte basic protein) and Mal (T-cell differentiation protein) did not produce signals. We noted that, as far as these genes were expressed and represented on the chips, they showed strong induction (Fig. 8), in agreement with the earlier OPC work. However, we also noted that plateau values were reached faster in Oli-neu cells than in the earlier work, peaking between 24 and 72 h in our study versus days 5 to 9 in a previous report (9). Also, all of the genes shown in Fig. 8 show fairly similar curves; segregation in presumed "early" and "late" sets (Fig. 8A and B, respectively) did not clearly resolve the curves. For instance, while Mbp is induced early in both studies, "late" gene Tspan2 only begins to be induced at day 3 and peaks at

FIG. 4. Induction of oligodendrocyte differentiation markers after siRNA-mediated silencing of genes in Oli-neu (3 days). Two different siRNAs were used for each gene (blue and pink bars). The positive control was ErbB2/Neu (green bars); the negative control (for ratio calculation) was luciferase siRNA. The data were combined from multiple experiments as indicated (e.g., two separate experiments using duplicates for panel A). The readouts were CNP enzymatic activity (A), MBP ELISA (B), PLP qPCR (C), MBP qPCR (D), CNP qPCR (E), and dendrocyte outgrowth (F) measured using O4-antibody staining (Cellomics). (G) Phase-contrast imaging of morphological changes accompanying Oli-neu differentiation as induced by siRNAs for indicated genes. Luciferase and Ptdss2 (top row) are inactive siRNAs.

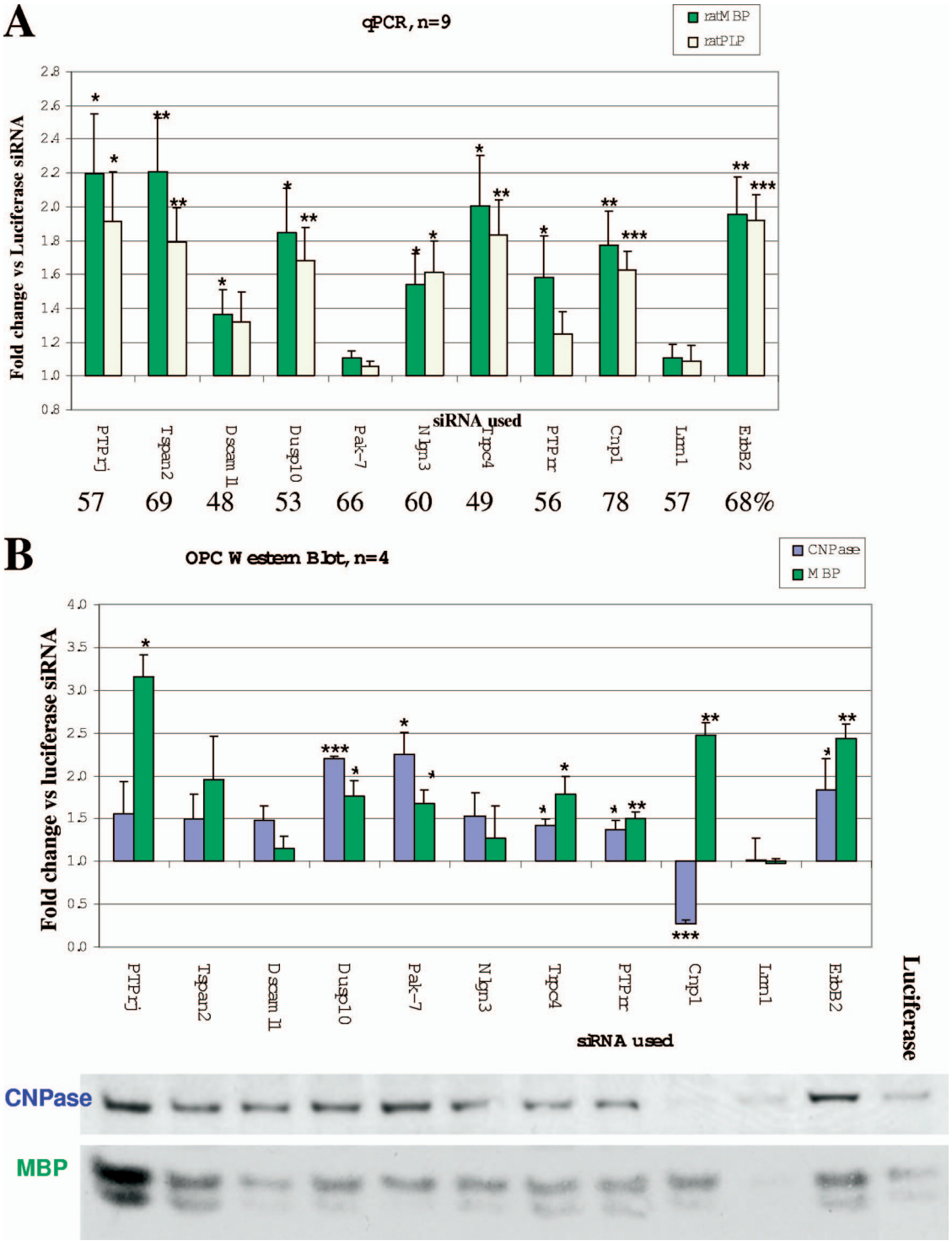

FIG. 5. RNAi-induced of differentiation of rat OPCs. The readouts were MBP and PLP mRNA induction as measured by qPCR (A) and MBP and PLP protein as measured by Western blotting (autoradiogram shown in lower panel) (B). mRNA knockdown achieved by the siRNAs (measured by qPCR) is indicated at the bottom of panel A. Statistical significance (versus the luciferase siRNA negative control): ***, $P < 0.001$; **, $P < 0.05$; *, $P < 0.1$.

day 9 in the study by Dugas et al. (9), whereas in our study (Fig. 8B) the Tspan2 curve shapes are very similar to those seen for the "early" Mbp probesets. It is possible that the ~10% of non-OPCs in the preparation used in the Dugas study provide negative-feedback signaling to the OPCs as they differentiate, slowing down and segregating differentiation into distinct processes. Combined with our results, this suggests that OPCs are subject to negative control in mixed cultures and probably in situ as well. Known examples for such inhibitors of differentiation include the Lingo1 receptor and its ligands NogoA, Mag

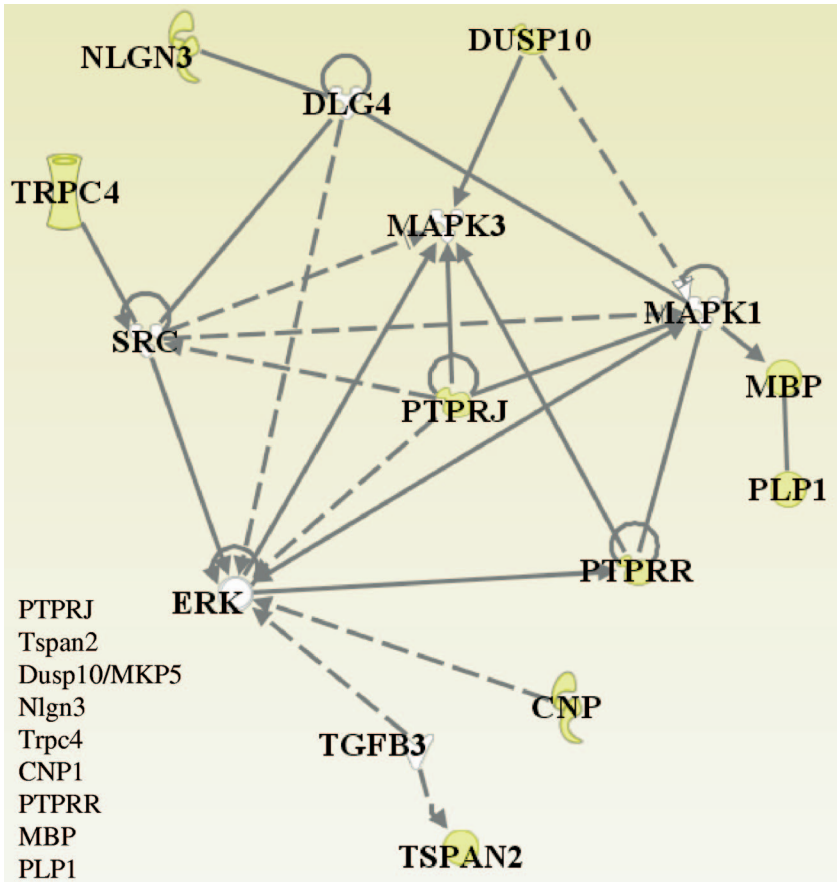

FIG. 6. Pathway mapping of OPC differentiation inducer genes. Genes for siRNAs that induced differentiation in Oli-neu and confirmed in OPCs (see the list) were groupwise analyzed in the context of established gene-gene interactions using Ingenuity Pathway analysis software. Lines correspond to direct (physical) interactions (enzyme-substrate, yeast two-hybrid, or immunoprecipitation; dashed lines represent indirect interactions, e.g., induction).

(myelin-associated glycoprotein), and Omgp (oligodendrocyte-myelin glycoprotein [recently reviewed in reference 28]).

DISCUSSION

The process whereby precursor cells differentiate into mature lineages is poorly understood. Recent work showed that this process can be experimentally induced through the activation or overexpression of single transcription factors, e.g., T_{bet} for Th1, GATA3 for Th2, RORα for Th17, and FoxP3 for T_{reg} cells in the immune system, while embryonic stem cells can be reprogrammed using defined sets of just a few transcription factors (reviewed in references 23 and 42). The oligodendrocyte lineage is under the control of Olig1/2; Sox (SRY-box containing gene) -5, -6, and -10; Oct6; and Nkx2.2 (NK2 homeobox 2) transcription factors (26, 42). How these transcription factors interact with environmental stimuli and cascade a myriad of transcriptional activities is poorly understood. The differentiation process has been viewed as one generating stable attractors from an uncommitted metastable state to another that involves the creation of autostimulation and cross-inhibition (15). Such a view is compatible with the generation of multiple redundant, negative controls seen in our Oli-neu study.

Our work focused on identifying relevant downstream effectors of OPC differentiation, starting out from comprehensive sets of genes that were regulated during Oli-neu differentiation as induced after treatment with various agents. We found that each differentiating treatment induced changes in expression in a characteristic set of genes and that only a small subset of these genes was shared between treatments. As differentiation progressed over time, however, the set of commonly modulated genes expanded.

The same data set can also be analyzed for genes that specifically associate with myelination, as opposed to process formation, which we examined earlier. We identified genes that were modulated by PD174265 (a treatment that resulted in MBP synthesis) but were not, or differently regulated by forskolin (which induced process, but not MBP formation). Analysis of the resulting gene set did not match to a single, well-characterized network, presumably because in this case we did not have a sufficiently large number of different treatments that would allow us to filter the gene sets.

Our results demonstrate that pure Oli-neu cells present an excellent model for oligodendrocyte differentiation, as witnessed by the induction of various myelin-associated markers and dendritic outgrowth. For instance, Tmem10/Opalin was

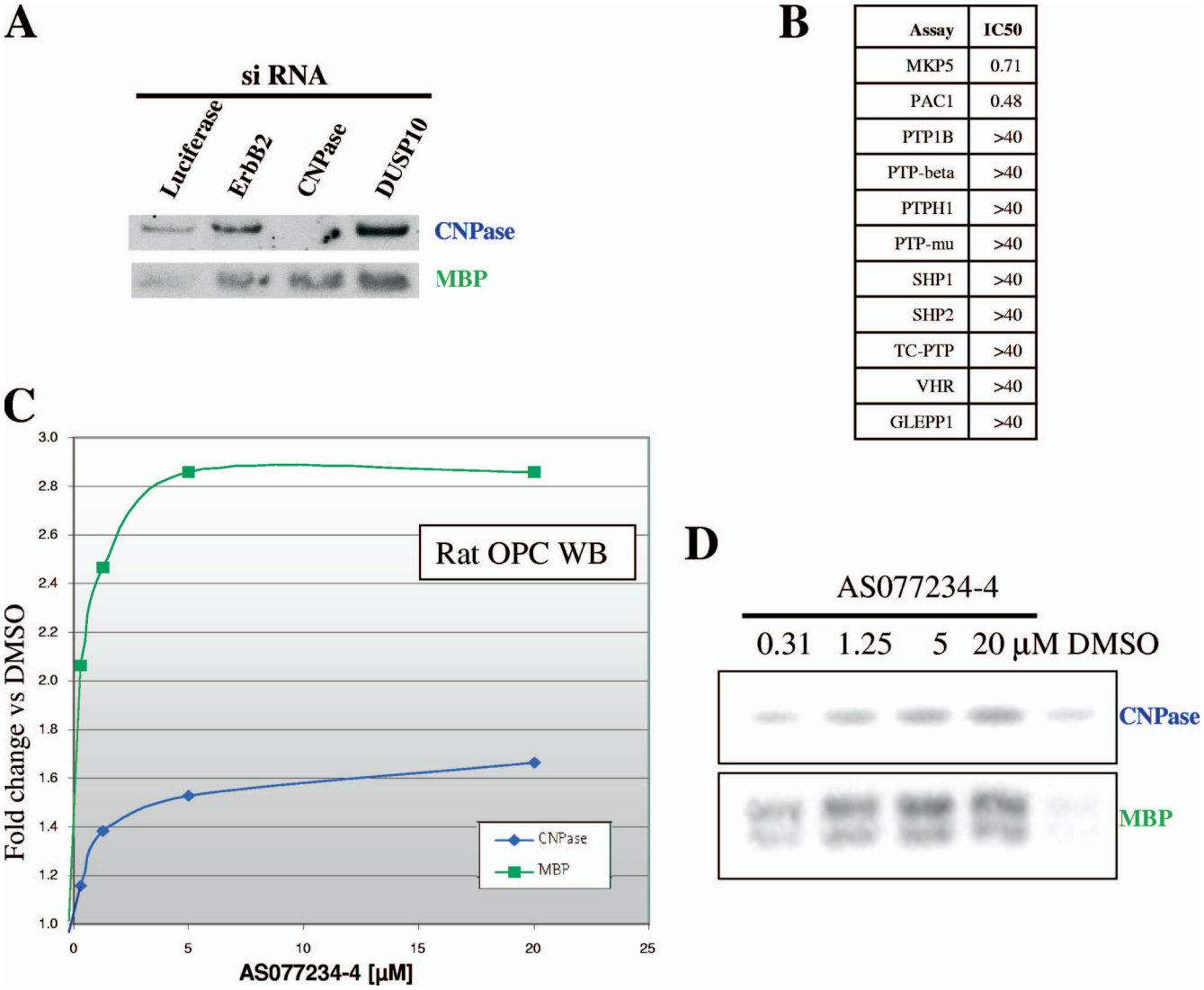

Assay	IC50
MKP5	0.71
PAC1	0.48
PTP1B	>40
PTP-beta	>40
PTPH1	>40
PTP-mu	>40
SHP1	>40
SHP2	>40
TC-PTP	>40
VHR	>40
GLEPP1	>40

FIG. 7. Induction of OPC differentiation using an enzymatic MKP5 inhibitor. (A) Potent induction of MBP and CNP by siRNA knockdown on MKP5 in OPCs. (B) Selectivity among protein tyrosine phosphatases of an organic, novel MKP5 inhibitor, AS077234-4 (IC_{50} given in μM). (C) Treatment of rat OPCs with AS077234-4 results in dose-dependent induction of MBP and CNP differentiation marker proteins. DMSO, negative control with compound solvent only. (D) Western blot used for the graphic representation (scan) of panel C.

recently identified as a novel oligodendrocyte differentiation marker (19), and this gene's expression increased 43-fold in PD174265-treated Oli cells. Likewise, known critical transcription factors Sox8 and -17 (reviewed in reference 42) were up- and downregulated, respectively, in our datasets, as described previously. Furthermore, we demonstrate that differentiation is under considerable negative control both in Oli-neu cells and in primary OPCs. An earlier example of oligodendrocyte negative control is Sirt2 (sirtuin 2), an oligodendroglial cell-specific gene whose repression results in CNP and MBP induction (24). It was proposed that Sirt2 functions "to prevent overdifferentiation or early aging of the [oligodendroglial] cells" (24). In our data set, Sirt2 gene expression is strongly induced by PD174265.

CNP, a well-studied constituent of uncompacted myelin, had not been identified earlier as (yet another) myelin component that inhibits oligodendrocyte differentiation. Mice that overexpress CNP lack myelin compaction and undergo precocious maturation (12, 43). Surprisingly, mice that lack CNP present normal myelin and yet undergo severe neurodegeneration due to "uncoupled oligodendrocyte functions" (21). Our work showing that CNP negatively regulates oligodendrocyte differentiation provides a basis for understanding these in vivo observations and reveals a role for CNP in appropriate timing and control of OPC differentiation.

The seven genes that we identified as autoinhibitory (listed in Fig. 6, along with MBP) are all expressed in various areas of the murine central nervous system (see the expression data in the supplemental material as retrieved from the Internet Allen Brain Atlas, which is described in reference 22)—with the exception of PTPRR, which is nevertheless known to play important neural functions (8). Among murine neural cell

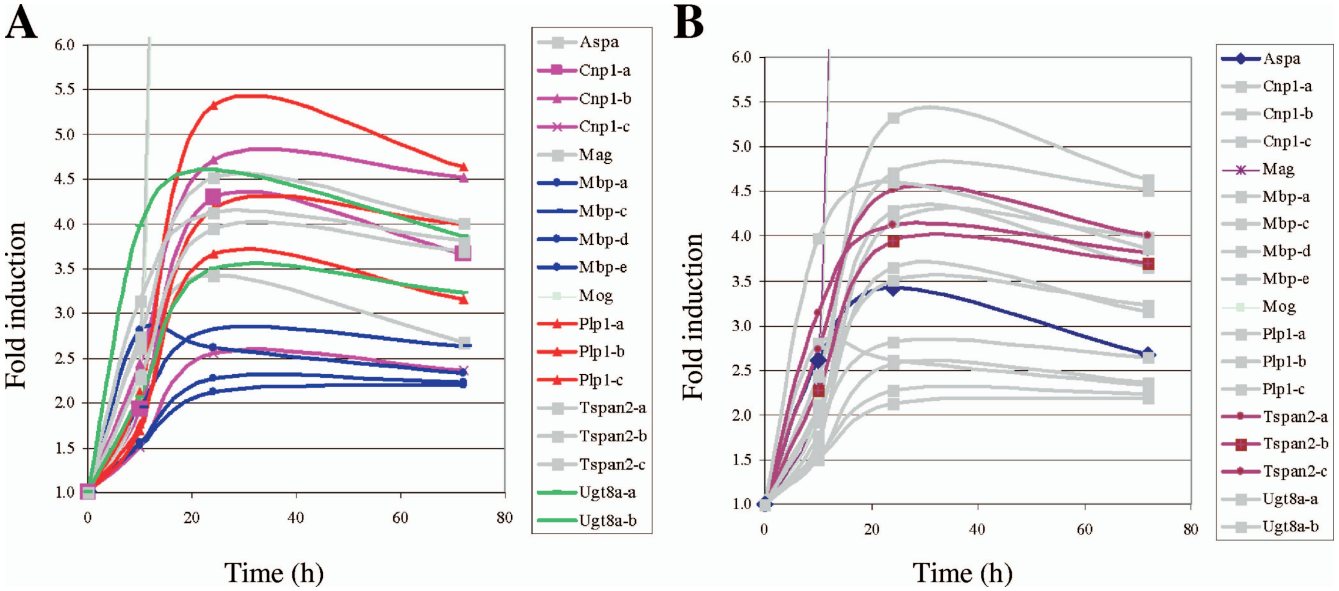

FIG. 8. Induction by PD174265 in Oli-neu of a subset of genes earlier identified (9) as "early" and "late" myelin genes in rat OPCs. "Early" genes are colored in panel A; "late" genes are colored in panel B. The suffixes "-a," "-b," and "-c" refer to different probe sets for the same gene. Induction for the Mag probe was off-scale, possibly due to off-target hybridization. The induction of all genes is highly significant ($P < 0.01$).

lines, PTPRJ, PTPRR, Dusp10, and Nlgn3 are all overexpressed in oligodendrocytes, whereas Tspan2 (tetraspanin 2) displays 28-fold increased expression in myelinating oligodendrocytes compared to OPCs (see reference 5 and online material associated with this reference).

Tspan2 has been discovered in an oligodendrocyte/OPC subtractive cDNA library (4) and was later postulated to represent "a molecular link between surface integrins and a CD9, Tspan-2 molecular web during the differentiation of oligodendrocytes" (39). Our results support models in which this complex is involved in cell-cell interactions that control oligodendrocyte differentiation.

Three of the other "repressors" that we identified are more usually associated with neurons: TRPC4 is a potential cation channel expressed in the developing (murine) brain (44), and Dscaml1 may, based on its expression pattern, be involved in formation and maintenance of neural networks (1). Nlgn3 is a neuron-specific adhesion molecule, mutations in which are associated with autism-spectrum disorders and mental retardation (7), diseases which have also been associated with abnormal myelination (10).

Three repressors (PTPRj, PTPRr, and MKP5) are protein tyrosine phosphatases, whose members are known to exert negative feedback on "forward" kinase phosphorylation cascades. For instance, PTP1B dampens insulin receptor signaling (reviewed in reference 14), while mice that lack PTPH1 display enhanced growth hormone sensitivity and systemic growth (34). PTPRj, also named density-enhanced phosphatase (DEP), has an antiproliferative effect (3), may use Erk1/2 as a substrate (27), and has been linked to cell adhesion (33). MKP5 inactivates p38 and JNK in vitro (38, 40), and PTPRr also inactivates Erk1/2. Mice that lack the *PTPRr* gene display impaired motor coordination (8). Thus, all PTPs that we identified here have earlier been shown to negatively regulate Erk1/2 signaling cascades. The Erk1/2 pathway has been implicated earlier in "promoting dedifferentiation of myelinating cells" (17). In a different context, Erk1/2 activating stimuli were recently shown to increase mRNA levels for eight DUSPs, and an siRNA screen showed that 12 of 16 DUSPs (including DUSP5) influence ERK2 responses (6).

Based on these recent observations, it appears plausible that the induction of PTP/DUSP mRNAs that we observed as a characteristic of early oligodendrocyte differentiation (shared by multiple treatments) may be a consequence of Erk activation and that interfering with induction of some of these PTP mRNAs prevents negative feedback to Erk signaling. Although genes that are activated during differentiation of oligodendrocytes or other cell types are often tacitly assumed to promote the differentiation process, our study indicates that the transcriptional machinery that drives differentiation also generates a number of "self-regulatory" transcripts that normally prevent cells from spontaneously changing their state.

Our finding that an MKP5 inhibitor induces OPC differentiation demonstrates that, at least for this gene, its "repressor function" is related to its enzymatic function. Earlier work on MKP5 knockout mice had shown that these animals show enhanced T-cell responses with increased production of Ifn-γ and tumor necrosis factor alpha upon lymphocytic choriomeningitis virus infection and yet were, perhaps surprisingly, partially protected from experimental autoallergic encephalitis (45). Our study opens the possibility that MKP5 knockout animals are (also) protected from disease through enhanced oligodendrocyte-mediated remyelination.

More generally, our experimental approach demonstrates how functionally relevant genes can be extracted from the thousands that are modulated in a typical differential gene expression experiment, by intersecting datasets obtained for phenotypically converging conditions.

ACKNOWLEDGMENTS

We thank Laurent Menoud for purifying the MKP5 enzyme; Artush Yeghiazaryan for compound management; Lionel Arnaud, Marie-José Frossard, Sandrine Pouly, Yves Sagot, and Arthur Roach for technical advice; Sandrine Pouly for artwork; Ewen Sedman for critically reading the manuscript; and Jacky Trotter for the Oli-neu cell line.

R.H.V.H. receives funding from the European Union Research Training Network MRTN-CT-2006-035830. AS077234 is available to members of the scientific community for noncommercial purposes upon request.

REFERENCES

1. **Agarwala, K. L., S. Ganesh, Y. Tsutsumi, T. Suzuki, K. Amano, and K. Yamakawa.** 2001. Cloning and functional characterization of DSCAML1, a novel DSCAM-like cell adhesion molecule that mediates homophilic intercellular adhesion. Biochem. Biophys. Res. Commun. **285:**760–772.
2. **Aston, C., L. Jiang, and B. P. Sokolov.** 2005. Transcriptional profiling reveals evidence for signaling and oligodendroglial abnormalities in the temporal cortex from patients with major depressive disorder. Mol. Psychiatr. **10:**309–322.
3. **Balavenkatraman, K. K., E. Jandt, K. Friedrich, T. Kautenburger, B. L. Pool-Zobel, A. Ostman, and F. D. Bohmer.** 2006. DEP-1 protein tyrosine phosphatase inhibits proliferation and migration of colon carcinoma cells and is upregulated by protective nutrients. Oncogene **25:**6319–6324.
4. **Birling, M. C., S. Tait, R. J. Hardy, and P. J. Brophy.** 1999. A novel rat tetraspan protein in cells of the oligodendrocyte lineage. J. Neurochem. **73:**2600–2608.
5. **Cahoy, J. D., B. Emery, A. Kaushal, L. C. Foo, J. L. Zamanian, K. S. Christopherson, Y. Xing, J. L. Lubischer, P. A. Krieg, S. A. Krupenko, W. J. Thompson, and B. A. Barres.** 2008. A transcriptome database for astrocytes, neurons, and oligodendrocytes: a new resource for understanding brain development and function. J. Neurosci. **28:**264–278.
6. **Caunt, C. J., S. P. Armstrong, C. A. Rivers, M. R. Norman, and C. A. McArdle.** 2008. Spatiotemporal regulation of ERK2 by dual specificity phosphatases. J. Biol. Chem. **283:**26612–26623.
7. **Chih, B., S. K. Afridi, L. Clark, and P. Scheiffele.** 2004. Disorder-associated mutations lead to functional inactivation of neuroligins. Hum. Mol. Genet. **13:**1471–1477.
8. **Chirivi, R. G., Y. E. Noordman, C. E. Van der Zee, and W. J. Hendriks.** 2007. Altered MAP kinase phosphorylation and impaired motor coordination in PTPRR deficient mice. J. Neurochem. **101:**829–840.
9. **Dugas, J. C., Y. C. Tai, T. P. Speed, J. Ngai, and B. A. Barres.** 2006. Functional genomic analysis of oligodendrocyte differentiation. J. Neurosci. **26:**10967–10983.
10. **Fields, R. D.** 2008. White matter in learning, cognition and psychiatric disorders. Trends Neurosci. **31:**361–370.
11. **Franklin, R. J., and M. R. Kotter.** 2008. The biology of CNS remyelination: the key to therapeutic advances. J. Neurol. **255**(Suppl. 1)**:**19–25.
12. **Gravel, M., J. Peterson, V. W. Yong, V. Kottis, B. Trapp, and P. E. Braun.** 1996. Overexpression of 2′,3′-cyclic nucleotide 3′-phosphodiesterase in transgenic mice alters oligodendrocyte development and produces aberrant myelination. Mol. Cell Neurosci. **7:**453–466.
13. **Han, M. H., S. I. Hwang, D. B. Roy, D. H. Lundgren, J. V. Price, S. S. Ousman, G. H. Fernald, B. Gerlitz, W. H. Robinson, S. E. Baranzini, B. W. Grinnell, C. S. Raine, R. A. Sobel, D. K. Han, and L. Steinman.** 2008. Proteomic analysis of active multiple sclerosis lesions reveals therapeutic targets. Nature **451:**1076–1081.
14. **Hooft van Huijsduijnen, R.** 2003. Drug discovery and development for metabolic diseases. Drug Discov. Today **8:**1064–1066.
15. **Huang, S., Y. P. Guo, G. May, and T. Enver.** 2007. Bifurcation dynamics in lineage-commitment in bipotent progenitor cells. Dev. Biol. **305:**695–713.
16. **Hudson, L. D.** 2003. Pelizaeus-Merzbacher disease and spastic paraplegia type 2: two faces of myelin loss from mutations in the same gene. J. Child Neurol. **18:**616–624.
17. **Jessen, K. R., and R. Mirsky.** 2008. Negative regulation of myelination: relevance for development, injury, and demyelinating disease. Glia **56:**1552–1565.
18. **Jung, M., E. Kramer, M. Grzenkowski, K. Tang, W. Blakemore, A. Aguzzi, K. Khazaie, K. Chlichlia, G. von Blankenfeld, H. Kettenmann, et al.** 1995. Lines of murine oligodendroglial precursor cells immortalized by an activated neu tyrosine kinase show distinct degrees of interaction with axons in vitro and in vivo. Eur. J. Neurosci. **7:**1245–1265.
19. **Kippert, A., K. Trajkovic, D. Fitzner, L. Opitz, and M. Simons.** 2008. Identification of Tmem10/Opalin as a novel marker for oligodendrocytes using gene expression profiling. BMC Neurosci. **9:**40.
20. **Kuhlmann, T., V. Miron, Q. Cuo, C. Wegner, J. Antel, and W. Bruck.** 2008. Differentiation block of oligodendroglial progenitor cells as a cause for remyelination failure in chronic multiple sclerosis. Brain **131:**1749–1758.
21. **Lappe-Siefke, C., S. Goebbels, M. Gravel, E. Nicksch, J. Lee, P. E. Braun, I. R. Griffiths, and K. A. Nave.** 2003. Disruption of Cnp1 uncouples oligodendroglial functions in axonal support and myelination. Nat. Genet. **33:**366–374.
22. **Lein, E. S., M. J. Hawrylycz, N. Ao, M. Ayres, A. Bensinger, A. Bernard, A. F. Boe, M. S. Boguski, K. S. Brockway, E. J. Byrnes, L. Chen, L. Chen, T. M. Chen, M. C. Chin, J. Chong, B. E. Crook, A. Czaplinska, C. N. Dang, S. Datta, N. R. Dee, A. L. Desaki, T. Desta, E. Diep, T. A. Dolbeare, M. J. Donelan, H. W. Dong, J. G. Dougherty, B. J. Duncan, A. J. Ebbert, G. Eichele, L. K. Estin, C. Faber, B. A. Facer, R. Fields, S. R. Fischer, T. P. Fliss, C. Frensley, S. N. Gates, K. J. Glattfelder, K. R. Halverson, M. R. Hart, J. G. Hohmann, M. P. Howell, D. P. Jeung, R. A. Johnson, P. T. Karr, R. Kawal, J. M. Kidney, R. H. Knapik, C. L. Kuan, J. H. Lake, A. R. Laramee, K. D. Larsen, C. Lau, T. A. Lemon, A. J. Liang, Y. Liu, L. T. Luong, J. Michaels, J. J. Morgan, R. J. Morgan, M. T. Mortrud, N. F. Mosqueda, L. L. Ng, R. Ng, G. J. Orta, C. C. Overly, T. H. Pak, S. E. Parry, S. D. Pathak, O. C. Pearson, R. B. Puchalski, Z. L. Riley, H. R. Rockett, S. A. Rowland, J. J. Royall, M. J. Ruiz, N. R. Sarno, K. Schaffnit, N. V. Shapovalova, T. Sivisay, C. R. Slaughterbeck, S. C. Smith, K. A. Smith, B. I. Smith, A. J. Sodt, N. N. Stewart, K. R. Stumpf, S. M. Sunkin, M. Sutram, A. Tam, C. D. Teemer, C. Thaller, C. L. Thompson, L. R. Varnam, A. Visel, R. M. Whitlock, P. E. Wohnoutka, C. K. Wolkey, V. Y. Wong, et al.** 2007. Genome-wide atlas of gene expression in the adult mouse brain. Nature **445:**168–176.
23. **Lewitzky, M., and S. Yamanaka.** 2007. Reprogramming somatic cells towards pluripotency by defined factors. Curr. Opin. Biotechnol. **18:**467–473.
24. **Li, W., B. Zhang, J. Tang, Q. Cao, Y. Wu, C. Wu, J. Guo, E. A. Ling, and F. Liang.** 2007. Sirtuin 2, a mammalian homolog of yeast silent information regulator-2 longevity regulator, is an oligodendroglial protein that decelerates cell differentiation through deacetylating α-tubulin. J. Neurosci. **27:**2606–2616.
25. **Lindberg, R. L., C. J. De Groot, U. Certa, R. Ravid, F. Hoffmann, L. Kappos, and D. Leppert.** 2004. Multiple sclerosis as a generalized CNS disease: comparative microarray analysis of normal appearing white matter and lesions in secondary progressive MS. J. Neuroimmunol. **152:**154–167.
26. **Liu, Z., X. Hu, J. Cai, B. Liu, X. Peng, M. Wegner, and M. Qiu.** 2007. Induction of oligodendrocyte differentiation by Olig2 and Sox10: evidence for reciprocal interactions and dosage-dependent mechanisms. Dev. Biol. **302:**683–693.
27. **Massa, A., F. Barbieri, C. Aiello, R. Iuliano, S. Arena, A. Pattarozzi, A. Corsaro, V. Villa, A. Fusco, G. Zona, R. Spaziante, G. Schettini, and T. Florio.** 2004. The phosphotyrosine phosphatase eta mediates somatostatin inhibition of glioma proliferation via the dephosphorylation of ERK1/2. Ann. N. Y. Acad. Sci. **1030:**264–274.
28. **Mi, S., A. Sandrock, and R. H. Miller.** 2008. LINGO-1 and its role in CNS repair. Int. J. Biochem. Cell. Biol. **40:**1971–1978.
29. **Mycko, M. P., R. Papoian, U. Boschert, C. S. Raine, and K. W. Selmaj.** 2004. Microarray gene expression profiling of chronic active and inactive lesions in multiple sclerosis. Clin. Neurol. Neurosurg. **106:**223–229.
30. **Nicolay, D. J., J. R. Doucette, and A. J. Nazarali.** 2007. Transcriptional control of oligodendrogenesis. Glia **55:**1287–1299.
31. **Oksenberg, J. R., S. E. Baranzini, S. Sawcer, and S. L. Hauser.** 2008. The genetics of multiple sclerosis: SNPs to pathways to pathogenesis. Nat. Rev. Genet. **9:**516–526.
32. **Pasquali, C., M. L. Curchod, S. Walchli, X. Espanel, M. Guerrier, F. Arigoni, G. Strous, and R. Hooft van Huijsduijnen.** 2003. Identification of protein tyrosine phosphatases with specificity for the ligand-activated growth hormone receptor. Mol. Endocrinol. **17:**2228–2239.
33. **Pera, I. L., R. Iuliano, T. Florio, C. Susini, F. Trapasso, M. Santoro, L. Chiariotti, G. Schettini, G. Viglietto, and A. Fusco.** 2005. The rat tyrosine phosphatase eta increases cell adhesion by activating c-Src through dephosphorylation of its inhibitory phosphotyrosine residue. Oncogene **24:**3187–3195.
34. **Pilecka, I., C. Patrignani, R. Pescini, M.-L. Curchod, D. Perrin, Y. Xue, J. Yasenchak, A. Clark, M. C. Magnone, P. Zaratin, D. Valenzuela, C. Rommel, and R. Hooft van Huijsduijnen.** 2007. Protein tyrosine phosphatase H1 (PTP-H1/PTPN3) controls growth hormone receptor signaling and systemic growth. J. Biol. Chem. **282:**35405–35415.
35. **Reich, D., N. Patterson, P. L. De Jager, G. J. McDonald, A. Waliszewska, A. Tandon, R. R. Lincoln, C. DeLoa, S. A. Fruhan, P. Cabre, O. Bera, G. Semana, M. A. Kelly, D. A. Francis, K. Ardlie, O. Khan, B. A. Cree, S. L. Hauser, J. R. Oksenberg, and D. A. Hafler.** 2005. A whole-genome admixture scan finds a candidate locus for multiple sclerosis susceptibility. Nat. Genet. **37:**1113–1118.
36. **Sommer, I., and M. Schachner.** 1981. Monoclonal antibodies (O1 to O4) to oligodendrocyte cell surfaces: an immunocytological study in the central nervous system. Dev. Biol. **83:**311–327.
37. **Stadelmann, C., and W. Bruck.** 2008. Interplay between mechanisms of damage and repair in multiple sclerosis. J. Neurol. **255**(Suppl. 1)**:**12–18.
38. **Tanoue, T., T. Moriguchi, and E. Nishida.** 1999. Molecular cloning and characterization of a novel dual specificity phosphatase, MKP5. J. Biol. Chem. **274:**19949–19956.
39. **Terada, N., K. Baracskay, M. Kinter, S. Melrose, P. J. Brophy, C. Boucheix, C. Bjartmar, G. Kidd, and B. D. Trapp.** 2002. The tetraspanin protein, CD9,

is expressed by progenitor cells committed to oligodendrogenesis and is linked to beta1 integrin, CD81, and Tspan-2. Glia **40:**350–359.

40. **Theodosiou, A., A. Smith, C. Gillieron, S. Arkinstall, and A. Ashworth.** 1999. MKP5, a new member of the MAP kinase phosphatase family, which selectively dephosphorylates stress-activated kinases. Oncogene **18:**6981–6988.
41. **Wälchli, S., M.-L. Curchod, R. Pescini Gobert, S. Arkinstall, and R. Hooft van Huijsduijnen.** 2000. Identification of tyrosine phosphatases that dephosphorylate the insulin receptor: a brute-force approach based on "substrate-trapping" mutants. J. Biol. Chem. **275:**9792–9796.
42. **Wegner, M.** 2008. A matter of identity: transcriptional control in oligodendrocytes. J. Mol. Neurosci. **35:**3–12.
43. **Yin, X., J. Peterson, M. Gravel, P. E. Braun, and B. D. Trapp.** 1997. CNP overexpression induces aberrant oligodendrocyte membranes and inhibits MBP accumulation and myelin compaction. J. Neurosci. Res. **50:**238–247.
44. **Zechel, S., S. Werner, and O. von Bohlen Und Halbach.** 2007. Distribution of TRPC4 in developing and adult murine brain. Cell Tissue Res. **328:**651–656.
45. **Zhang, Y., J. N. Blattman, N. J. Kennedy, J. Duong, T. Nguyen, Y. Wang, R. J. Davis, P. D. Greenberg, R. A. Flavell, and C. Dong.** 2004. Regulation of innate and adaptive immune responses by MAP kinase phosphatase 5. Nature **430:**793–797.